Published April 1, 1994

Ultrastructure of the Yeast Actin Cytoskeleton and Its Association with the Plasma Membrane

Jon Mulholland,* Daphne Preuss,‡ Anne Moon,§ Amie Wong,* David Drubin,§ and David Botstein*

*Department of Genetics and ‡Department of Biochemistry, Beckman Center, Stanford University Medical Center, Stanford, California 94305; and §Department of Molecular and Cell Biology, University of California, Berkeley, California 94720

Abstract. We characterized the yeast actin cytoskeleton at the ultrastructural level using immunoelectron microscopy. Anti-actin antibodies primarily labeled dense, patchlike cortical structures and cytoplasmic cables. This localization recapitulates results obtained with immunofluorescence light microscopy, but at much higher resolution. Immuno-EM double-labeling experiments were conducted with antibodies to actin together with antibodies to the actin binding proteins Abplp and cofilin. As expected from immunofluorescence experiments, Abplp, cofilin, and actin colocalized in immuno-EM to the dense patchlike structures but not to the cables. In this way, we can unambiguously identify the patches as the cortical actin cytoskeleton. The cortical actin patches were observed to be associated with the cell surface via an invagination of plasma membrane. This novel cortical cytoskeleton-plasma membrane interface appears to consist of a fingerlike invagination of plasma membrane around which actin filaments and actin binding proteins are organized. We propose a possible role for this unique cortical structure in wall growth and osmotic regulation.

INTERACTIONS between the plasma membrane and the actin cytoskeleton are involved in many diverse functions in eukaryotic cells, including development and control of cell morphology and polarity, adhesion to surfaces, membrane stability (particularly at areas of localized growth), and membrane domain organization (reviewed in Luna and Hitt, 1992). In the budding yeast *Saccharomyces cerevisiae*, the actin cytoskeleton has been implicated by its organization and mutant phenotypes in the development and maintenance of polarized growth (reviewed in Barnes et al., 1990; and Drubin, 1991).

The yeast actin cytoskeleton, in immunofluorescence light microscopy, appears as brightly staining cytoplasmic cables and cortical patches asymmetrically organized along the axis of cell growth (Adams and Pringle, 1984; Kilmartin and Adams, 1984; Novick and Botstein, 1985). Cortical actin patches are concentrated in areas of active cell growth and wall deposition within the bud. Actin cables are localized within both the mother and bud along the mother-daughter cell axis. Early in the cell cycle, a ring of actin patches appears upon the surface of the mother cell, marking the position from which the new bud will emerge. During bud emergence, this ring of actin patches persists, defining the neck of the small bud. As the bud enlarges, the ring of actin patches is lost and cortical actin patches become localized predominantly at the tip and sides of the now medium-sized bud. Late in the cell cycle, the actin patches appear randomly dispersed over the surface of the large bud and mother cell. During cytokinesis, cortical actin patches again are concentrated in the neck region, where septum formation occurs.

Many yeast actin binding proteins have been isolated and characterized using genetic and biochemical methods. Immunofluorescence light microscopy localization of these yeast actin binding proteins showed association with actin in vivo, but often also revealed differential localization to actin cables or cortical patches. For example, the nonessential actin binding protein Abplp, as well as the essential actin filament severing protein cofilin, are localized to cortical actin patches and not to actin cables (Drubin et al., 1988; Moon et al., 1993). Tropomyosin, which binds to filamentous actin in a divalent cation-dependent manner, is localized to cables of actin but not to cortical patches (Liu and Bretscher, 1989). In contrast, Sac6p, the yeast homologue of the vertebrate actin filament bundling protein fimbrin, always colocalizes with actin; i.e., to both the cables and cortical patches (Drubin et al., 1988; Adams et al., 1991) of the actin cytoskeleton. Genetic analysis has shown that each of these proteins makes unique contributions to the function of the actin cytoskeleton.

Differential localization of actin-binding proteins to cortical actin patches vis a vis cables suggests these distinct structures may play different roles in mediating the many physiological functions associated with the actin cytoskeleton.

Address all correspondence to David Botstein, Department of Genetics, Stanford University Medical Center, 300 Pasteur Drive, Stanford, CA 94305-5120.

Published April 1, 1994

While immunofluorescence studies have produced a wealth of data about the spatial and temporal localization of the actin cytoskeleton, these studies are limited by the small size of the yeast cell relative to the resolution of the light microscope. For these reasons, we have undertaken to study the morphology and molecular organization of the actin cables and cortical patches in the electron microscope. Previously, we developed and reported an improved immunoelectron microscopy technique that we used to identify and characterize the yeast endoplasmic reticulum and Golgi apparatus (Preuss et al., 1991 and 1992). Further development of this method has now allowed us to visualize and identify morphological elements of the yeast actin cytoskeleton in the electron microscope. In wild-type yeast cells, we have found that the cortical actin patch consists of an invagination of the plasma membrane, around which actin and associated proteins are organized.

Materials and Methods

Yeast Strains and Growth Conditions

The haploid yeast strain DBY1034 (*MATa his4-539 lys2-801 ura3-52 gal2*) is a wild-type strain (except for the auxotrophic markers) that is a direct descendant of strain S288C. DBY1034 was grown at 30°C in yeast-extract peptone medium (Sherman et al., 1986) containing glucose.

Immunoelectron Microscopy Methods: Overview

In keeping with the convention we established previously (Preuss et al., 1992), we have continued to number our methods sequentially. In this study, two new methods, Methods III and IV, were used to produce the yeast cell sections used in characterizing the actin cytoskeleton. Method III (see Figs. 4 and 8) produces a better preserved ultrastructure, particularly with respect to the endoplasmic reticulum and Golgi apparatus membranes, than did our previous methods (Preuss et al., 1991 and 1992). However, it also produces a dense cytoplasm and, therefore, the actin cytoskeleton appears less dense relative to the surrounding ribosome-dense cytoplasm. Method IV (see Figs. 3, 5, 6, 7, and 9) is the same as Method III, except that a weaker fixation of the cells is used. The resulting increased extraction of the cytoplasm relative to Method III allows the proteins of the actin cytoskeleton to appear more dense than the surrounding cytoplasm. A reduction in nonspecific localizations of anti-actin guinea pig serum, as well as an apparent increase in the localization signal using antibodies to Abp1p and cofilin also was observed using the weaker fixation of Method IV.

Fixation and Processing: Methods III and IV

A 100-ml culture of exponentially growing cells (5×10^6 cells/ml) in yeast extract peptone-2% glucose medium was quickly harvested by vacuum filtration over a 0.45-μm nitrocellulose membrane; filtration was stopped when the total volume in the filter apparatus was ~5 ml. To this concentrated cell suspension, still on the filter membrane, 25 ml of freshly prepared room temperature fixative (40 mM potassium phosphate, pH 6.7, 1 M sorbitol, and 3% [6% in Method IV] methanol-free formaldehyde [Glauert, A. M. 1975] freshly prepared from paraformaldehyde [Polysciences, Inc., Warrington, PA], 0.5% [0.2% in Method IV] glutaraldehyde [EM grade; Polysciences, Inc.], 1 mM $MgCl_2$, 1 mM $CaCl_2$) was added and mixed rapidly with the cells by pipetting the suspension several times. The cell suspension was then transferred to a 50-ml polypropylene centrifuge tube and incubated at room temperature for 1 h. The aforementioned differences in fixative are the only differences between Methods III and IV.

The fixed cells were then centrifuged at low speed in a clinical centrifuge and the pellet was resuspended in 25 ml 40 mM potassium phosphate buffer (pH 6.7) containing 0.75 M sorbitol. The cells were again centrifuged and washed two more times in 40 mM potassium phosphate buffer (pH 6.7) containing first 0.50 M sorbitol and then 0.25 M sorbitol. A final wash in 5 ml of 40 mM potassium phosphate buffer (pH 6.7) was performed, and the fixed cells were transferred to a glass (13 × 100 mm) test tube. As described previously (van Tuinen and Riezman, 1987), the final pellet of fixed cells was resuspended in 5 ml 1% sodium metaperiodate, incubated for 10 min at room temperature, and then centrifuged and resuspended in 5 ml distilled water. Next, the cells were centrifuged, resuspended in 5 ml 50 mM ammonium chloride, and incubated for 15 min at room temperature.

Before dehydration, the cells were washed once in distilled water, centrifuged at low speed, and then dehydrated (on ice) by resuspending the cell pellet in 30% (vol/vol) ice-cold ethanol and incubating on ice for 5 min. The cells were similarly centrifuged and sequentially resuspended in 50, 70, 80, 85, 90, and 95% ice-cold ethanol, and finally twice in 100% ice-cold ethanol. A final dehydration and centrifugation in 100% ethanol at room temperature was performed. The dehydrated cells then were infiltrated with room temperature L. R. White resin (Polysciences, Inc.) and prepared for polymerization as described by Wright and Rine (1989), except that infiltration of resin into the cells was done without application of vacuum and harvesting of cells was by centrifugation. The resin was polymerized by incubation at 47°C for 48 h.

Thin sections measuring ~40–50 nm (as determined by a gray/silver interference color) were cut with a diamond knife and were picked up on 300 mesh nickel grids (Polysciences Inc.) that had been made sticky with a dilute formvar solution (Wright and Rine, 1989). Serial sections consisting of 25–30 sections (40–50 nm thick) per ribbon were picked up with copper wire loops covered with formvar film and transferred under a dissecting microscope to nickel, 1 × 2-mm slotted grids (Ted Pella, Redding, CA). Slotted grids carrying serial sections were lightly carbon coated on the formvar film side, thereby leaving one side of the serially cut sections exposed for use in immunolocalization experiments described below. The formvar film on one side of the serial sections reduced the antibody signal to ~50% of the antibody signal obtained on nonserial sections that have both sides exposed. The contrast and resolution of serially sectioned cells was also less than that observed on nonserially sectioned cells, again because of the presence of the formvar film. For these reasons, we used nonserial sections whenever three-dimensional analysis was not required.

Double Labeling

We used extensively a double-labeling technique that depends on the use of primary antibodies from different species. To this end, anti-actin antibodies were prepared in guinea pigs. All the double-label experiments used the guinea pig serum; all the other experiments used affinity-purified anti-actin antibody raised in rabbits, which shows superior specificity.

Preparation of Anti-actin Antisera in Guinea Pigs

Yeast actin was produced and purified using the Zechel (1980) DNase I affinity purification procedure as modified by Drubin et al. (1988). The isolated actin appeared as a single band when visualized on Coomassie blue–stained SDS gels. Purified actin was dialyzed against PBS buffer for 24 h at 4°C, after which SDS was added to a final concentration of 0.1%. The denatured, purified actin was then frozen in liquid nitrogen and stored at −70°C.

To obtain polyclonal antibodies, the purified denatured actin was mixed with MPL (monophosphoryl lipid A) and TDM (trehalose dimycolate) adjuvant (Ribi ImmunoChem Research, Inc., Hamilton, MT) following the manufacturer's instructions to a final concentration of 44 μg/ml. 500 μl (22 μg actin) of this adjuvant-protein mixture was boiled, cooled on ice, and injected into each of four guinea pigs. Animals were injected with this same preparation of protein and adjuvant on days 20, 35, and 60. A first test bleeding was conducted on day 71. Antisera from all four guinea pigs tested positive when immunoblotted to polyvinyldifluoride membrane strips (Immobilon; Millipore Corp., Bedford, MA) containing total yeast cell extract or purified yeast actin that had been transferred from an SDS-polyacrylamide gel (Burnette, 1981). Immunodetection was accomplished using horseradish peroxidase–conjugated protein A (Cappel Laboratories, Cochranville, PA) with the enhanced chemiluminescence Western blotting detection system (Amersham Corp., Arlington Heights, IL). On day 93, the guinea pigs were again boosted and then exsanguinated on day 104. The resulting sera were stored at −30°C and retested for specificity as above.

Western blot analysis of preimmune and immune whole sera from several guinea pigs showed specificity for actin. Fig. 1 shows the Western blot results for the serum used throughout. Fig. 2 shows that this antiserum, without further purification, stains both the cables and cortical patches characteristic of the yeast actin cytoskeleton. In immunoelectron microscopy control experiments, this guinea pig anti-actin serum showed no cross-reactivity with the primary antibodies (raised in rabbits) directed against the actin binding proteins or with the anti-rabbit collodial gold secondary anti-

Published April 1, 1994

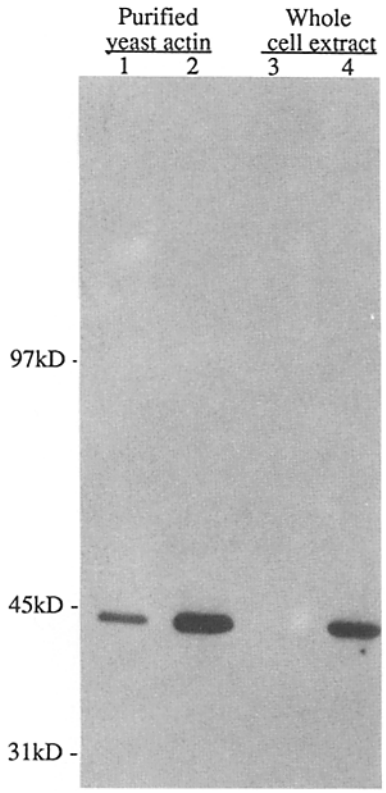

Figure 1. Immunoblot analysis of anti-actin guinea pig serum. Lanes *1* and *2* contain purified yeast actin (0.12 μg/lane) immunoblotted with affinity purified rabbit antibodies directed against yeast actin (diluted 1/1,000; lane *1*) and anti-actin serum from Guinea pig (diluted 1/1,000; lane *2*). Lanes *3* and *4* contain whole yeast cell extract immunoblotted with preimmune guinea pig serum (lane *3*, diluted 1/1,000) and anti-actin serum from guinea pig (lane *4*, diluted 1/1,000).

bodies. However, immunoelectron microscopy did reveal some minimal reactivity of the guinea pig serum with the yeast cell wall. This reactivity was reduced by preabsorption of the anti-actin guinea pig serum to fixed whole yeast cells (see below).

Production, purification, and characterization of affinity-purified, polyclonal rabbit antibodies to actin and Abplp have been described previously (Drubin et al., 1988), as have antibodies to cofilin (Moon et al., 1993).

Immunolabeling and Electron Microscopy

Antibody incubations were performed as previously described (Preuss et al., 1991). All antibodies were diluted in PBST (140 mM NaCl, 3 mM KCl, 8 mM Na_2HPO_4, 1.5 mM KH_2PO_4, and 0.05% Tween 20) containing 0.5% BSA and 0.5% ovalbumin (Sigma Immunochemicals, St. Louis, MO) and were incubated with cell sections mounted on grids as described above. Anti-actin antibodies (rabbit) were diluted 1:20, anti-Abplp antibodies were diluted 1:10, and anti-cofilin antibodies were diluted 1:40.

Anti-actin guinea pig serum was preabsorbed to fixed whole yeast cells before use in immuno-EM. Fixed whole yeast cells were prepared by fixing 4 ml of a saturated culture of DBY1034 in 4% glutaraldehyde (EM grade; Polysciences) at room temperature for 4 h. The fixed cells were then washed five times in 10 ml PBS (140 mM NaCl, 3 mM KCl, 8 mM Na_2HPO_4, and 1.5 mM KH_2PO_4) and finally resuspended in 2 ml of PBS. Preabsorption was accomplished by incubating equal volumes of fixed cells and anti-actin serum together at room temperature for 15 min. The cells were then removed by centrifugation. The preabsorbed, anti-actin whole guinea pig serum was diluted in PBST, 0.5% BSA, and 0.5% ovalbumin to a final concentration of 1/150.

The 10- and 20-nm gold-conjugated anti-rabbit IgG (goat) and anti-guinea pig IgG (goat) secondary antibodies (BioCell, Cardiff, United Kingdom) were all diluted 1:50 in PBST, 0.5% BSA, and 0.5% ovalbumin. In double labeling control experiments, the anti-guinea pig secondary antibodies showed no specificity for primary antibodies (anti-Abplp and anti-cofilin) raised in rabbit and anti-rabbit secondary antibodies did not react with the primary antibodies raised in guinea pig (anti-actin).

After immunolocalization the cell sections were postfixed in 8% glutaraldehyde (EM grade; Polysciences) for 30 min to prevent loss of antibody localization during subsequent high pH, lead citrate staining (see below). Cell sections were then washed by passing the grid, with slow slicing motion, through 500 ml of distilled water for 1 min. Postfixation of immunolocalized sections was not done for cells that were serially sectioned. All cell sections were poststained with 2% aqueous uranyl acetate (Polysciences, Inc.) for 1 h, washed as above for 30 s and dried on hardened filter paper for 5 min. Final poststaining was with 0.4% lead citrate as described by Reynolds (1963), for 15–30 s. Grids were washed as described above for 10–30 s and dried before examination in the electron microscope.

All observations were made on an electron microscope (model 300; Phillips Electronic Instruments Co., Mahwah, NJ) at an accelerating voltage of 80 kV using a 20-μm diameter objective aperture.

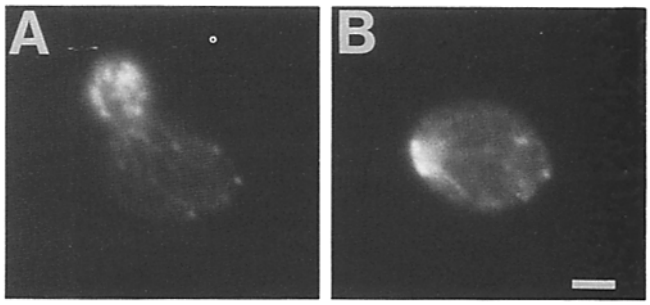

Figure 2. Immunofluorescence staining pattern of anti-actin guinea pig serum in yeast cells. The anti-actin serum localizes the cables and cortical patches of actin cytoskeleton. (*A*) Asymmetrical distribution of brightly staining actin structures in a budded cell. (*B*) Visualization of a ring of cortical patches at the presumptive site of bud emergence. Bar indicates 2.5 μm.

Immunofluorescence Light Microscopy

A growing culture of strain DBY1034 was fixed by direct addition of an equal volume of 10% methanol-free formaldehyde (Polysciences, Inc.). After a 30-min fixation at room temperature, the cells were washed and processed for immunofluorescence light microscopy according to Pringle et al. (1989). For immunofluorescence light microscopy, guinea pig anti-actin serum (with no preabsorption with whole cells; see above) was diluted in PBST (140 mM NaCl, 3 mM KCl, 8 mM Na_2HPO_4, 1.5 mM KH_2PO_4, and 0.05% Tween 20) containing 0.5% BSA and 0.5% ovalbumin to a final concentration of 1/2,000. Fluorescein-conjugated goat, anti-guinea pig secondary antibody (Cappel Laboratories) was diluted to a final concentration of 1/1,000 in the same diluent.

Results

Immunofluorescence studies showed that the yeast actin cytoskeleton consists of two types of actin-containing structures: cortical patches, which are concentrated at areas of active cell growth; and cables, which are aligned along the axis of cell growth (Adams and Pringle, 1984; Kilmartin and Adams, 1984; Novick and Botstein, 1985). To characterize these structures at the ultrastructural level, we used affinity-purified antibodies to immunolocalize actin in thin sections of wild-type yeast cells. Initial immunoelectron microscopic characterization of the yeast actin cytoskeleton revealed actin containing structures suggestive of both the actin cables and cortical patches defined by immunofluorescence micros-

Published April 1, 1994

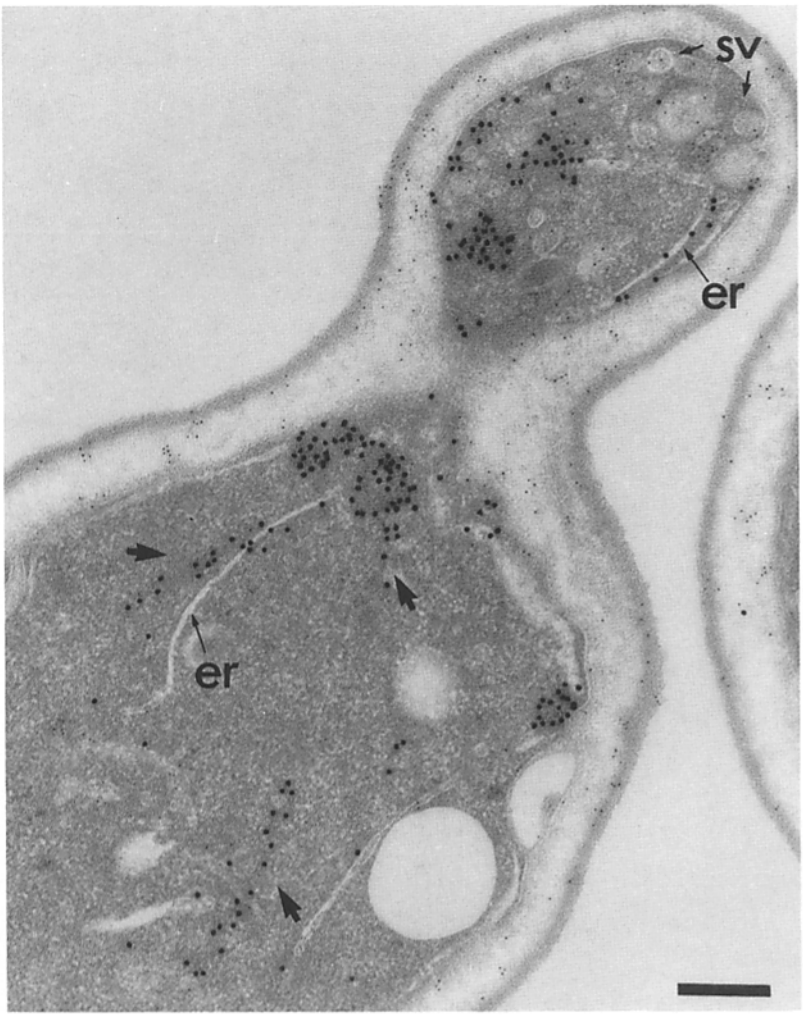

Figure 3. Immunogold localization of affinity-purified antibodies directed against actin. Dense patchlike localizations of 15-nm gold particles can be observed at the base of the bud neck, as well as within the bud. Cytoplasmic tracks of localization to actin cables (*large arrows*) can be observed running along the mother-daughter cell axis. Disperse localizations are visible within the bud, particularly along the bud periphery and the endoplasmic reticulum. Small gold (5 nm) is localization of concanavalin A. *er*, endoplasmic reticulum; *sv*, secretory vesicles. *Bar*, 0.25 μm.

copy (Fig. 3). In the electron microscope, actin cables were seen as thin extended electron-dense structures in the cytoplasm to which anti-actin antibodies were abundantly localized. These electron-dense cables were aligned along the axis of cell growth. The cortical patches were seen as electron-dense patches near the cell surface to which anti-actin antibodies were also abundantly localized.

Morphological Changes in the Actin Cytoskeleton during the Cell Cycle

Immunofluorescence light microscopy studies have shown that the structures of the yeast actin cytoskeleton, particularly the cortical patches, are distributed in a characteristic defined manner through the yeast cell cycle. Preservation of this cell cycle-dependent distribution of actin structures for microscopic examination depends on fixation conditions and is easily perturbed (reviewed in Pringle et al., 1989). Therefore, to determine whether the fixation methods used for our immuno-EM studies preserved the spatial and temporal organization of the actin cytoskeleton, the location and relative distribution of cortical actin patches was examined in cells at various points of the cell cycle. Asynchronous cell cultures were used to produce our immuno-EM sections; therefore, it was necessary to determine a cell's point in the cell cycle. We did this by comparing mother and bud size relative to neck diameter, as well as by examining the presence and distribution of characteristic organelles within the bud.

S. cerevisiae cells grow via localized fusion of secretory vesicles to the plasma membrane (Field and Schekman, 1980), and newly initiated buds can be identified easily by the clustering of these 50–70-nm secretory vesicles (Matile et al., 1969; Byers, 1981; Preuss et al., 1992). In these small budded cells a ring of dense actin patches was observed within the mother cell at the base of the bud neck (Fig. 4 *A*). This same ring of actin patches was observed by immunofluorescence light microscopy (Adams and Pringle, 1984; Novick and Botstein, 1985). Cross-sections through these actin patches showed them to contain electron-translucent cores, while longitudinal sections through apparently equivalent structures revealed characteristic invaginations of the cell surface surrounded by actin (Fig. 4, *A* and *B*). Antibodies directed against actin also localized within the vesicle-filled small bud, but this localization was disperse and not in patches.

At the stage of growth when organelles just begin to enter the small bud, dense actin localization within the bud was observed. This dense localization of actin made it difficult to determine if the antibody localization was primarily to actin patches, cables, and/or nonfilamentous actin. In medium-sized buds, the number of observable 50–70-nm vesicles

Published April 1, 1994

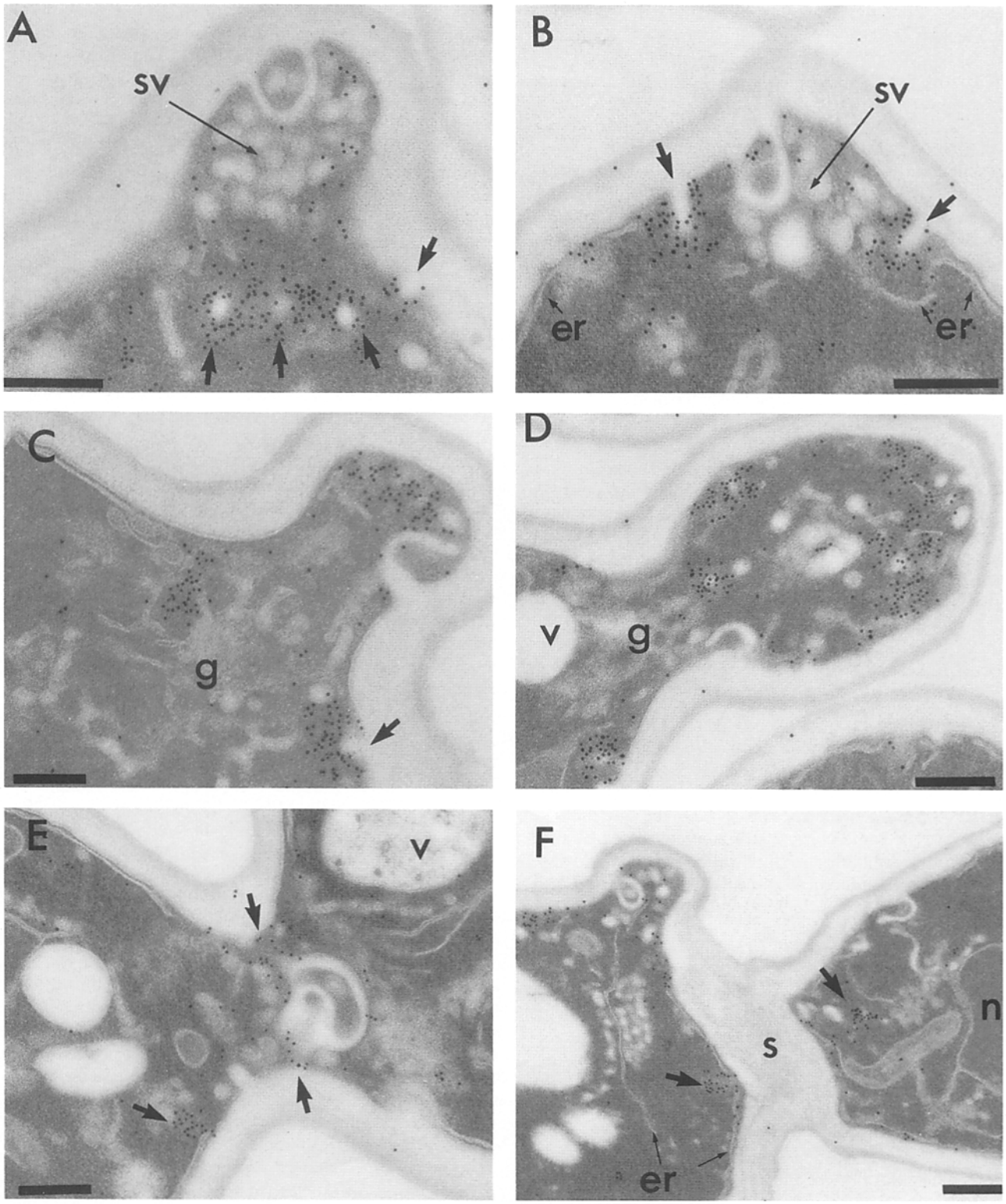

Figure 4. Immunolocalization of actin through the yeast cell cycle. On small budded cells (*A* and *B*), 10 nm gold particles label a ring of cortical actin patches positioned at the base of the bud neck. Immunogold localized cortical patches surround either an electron-translucent core or a cell surface invagination that do not label with anti-actin antibodies. Some disperse localization to the sides of the bud can also be observed. Cortical actin patches localize predominately to the tip, as well as to the sides of medium-sized bud (*C* and *D*). Late in the cell cycle, cortical actin patches were localized randomly to the surface of the mother and large bud, and they were concentrated at the site of septum formation (*E* and *F*). An apparent band of actin was observed at the neck during cytokinesis (*E*). *Large arrows*, cortical actin patches; *g*, Golgi; *n*, nucleus; *s*, septum; *v*, vacuole. *Bars*, 0.25 μm.

Published April 1, 1994

diminishes, and Golgi structures, followed by the endoplasmic reticulum, enter the neck and body of the bud (Preuss et al., 1991, 1992). Within such medium-sized buds (Fig. 4, *C* and *D*), discrete dense, patchlike localizations of anti-actin antibodies were observed at the bud tip and sides.

Large buds are marked by the presence of mitochondrial, vacuolar, and nuclear structures, as well as partial or complete septation (Matile et al., 1969; Byers, 1981; reviewed in Yaffe, 1991). In immuno-EM large budded cells that had not yet begun cytokinesis had actin patches localized primarily to their tips and occasionally along their sides. During cytokinesis, actin patches were localized over the surface of the mother and bud, and they were concentrated at the site of septum formation (Fig. 4, *E* and *F*).

Throughout the yeast cell cycle, cortical actin patches were observed in mother cells, but less frequently than in the buds and in an apparently random distribution. Actin antibodies sometimes localized to the cytoplasmic face of the endoplasmic reticulum, Golgi apparatus, and mitochondria in both mothers and buds. This localization to cytoplasmic membranes consisted primarily of disperse localizations and was never as prominent as that observed to the dense cortical patches. Some cytoplasmic localization of actin antibodies was observed.

These observations of actin localization, particularly to cortical patches, through the yeast cell cycle, were completely consistent with the localization patterns seen previously in immunofluorescence studies.

Colocalization of Actin and Actin Binding Proteins to the Cortical Actin Cytoskeleton

The actin binding proteins Abplp and cofilin have been shown by indirect immunofluorescence light microscopy to colocalize exclusively with the cortical actin cytoskeleton (Drubin et al., 1988; Moon et al., 1993). To confirm that the dense, cortical actin patches observed in the electron microscope are the same cortical structures observed by immunofluorescence, affinity-purified antibodies to Abplp and cofilin along with antibodies against actin were used in immunoelectron microscopy double-labeling experiments. Because the actin antibodies used in our initial characterization of the actin cytoskeleton were raised in the same animal (rabbit) as those antibodies directed against the actin binding proteins, it was necessary to raise new antibodies against actin in guinea pigs (see Materials and Methods).

Abplp and cofilin were found to colocalize with actin to the dense cortical patches (Figs. 5 and 6). Putative longitudinal and cross-sections (Fig. 7) through these dense patches revealed a core to which Abplp and cofilin, like actin, failed to localize. This core was clearly bounded by either a ring of membrane or by an invagination of plasma membrane, beyond which lay the electron dense material to which Abplp and cofilin clearly colocalized with actin.

Because the cell sections used in these double labeling experiments (made with Method IV) produced an electron-dense cytoskeleton relative to the cytoplasm, it was possible to observe the cables and the patches of the actin cytoskeleton both by the localization of gold-labeled antibodies and by the distinct appearance of the cytoskeletal structures. This is shown in Fig. 5, *A* and *B*, which show cortical actin patches that are both electron dense and immunolabeled with anti-actin and anti-Abplp antibodies. Observation of these cortical actin patches reveals each of them to be proximal and possibly even contiguous with an electron-dense cable that is clearly immunolabeled with actin antibodies (small gold particles) but not Abplp antibodies (large gold particles). An analogous image can be seen in Fig. 6 *A*, which shows immunolocalization of actin and cofilin; here again, the actin antibodies label both the cortical patches and the cables, but the cofilin antibodies label the patches only. Interestingly, actin cables appeared tangentially associated with cortical actin patches producing a characteristic "bent elbow" appearance.

Association of Cortical Actin Patches with the Plasma Membrane

We examined serially sectioned yeast cells to determine whether the actin patches containing a central membrane-bound core (referred to above as "cross-sections") and those that were associated with obvious invaginations of plasma membrane (the "longitudinal sections" above) were indeed identical structures seen from different aspects. Fig. 8 shows a typical series of sequential sections wherein it can be seen that the same structure that first appears as a longitudinal section, appears as a cross-section later in the series.

The serial section results, together with the individual images like the ones shown earlier, show that the plasma membrane invaginations are fingerlike projections that are completely surrounded by material that is labeled with anti-actin, anti-Abplp, and anti-cofilin antibodies. These fingerlike projections of plasma membrane often appear to turn from their original plane of invagination. Plasma membrane associated actin patches could be followed through an average of four to five serial sections. Assuming a section thickness of ~40–50 nm, these plasma membrane invaginations penetrate 150–250 nm into the interior of the cell. The diameter of the membrane bound core of the actin patch measures ~35–45 nm, and the diameter of the actin patch, in cross-section, is ~150 nm.

It is worth noting also that many prominent invaginations of plasma membrane, primarily observed in mother cells, but also along the sides of medium-sized or large buds, did not label with antibodies directed against actin. These plasma membrane invaginations were of variable length, and in serial sections, they appeared as furrows along the cell surface. In small buds, characteristically filled with 50–70-nm secretory vesicles, flattened invaginations of membrane, possibly the result of fusion events between the vesicles and the plasma membrane, also were observed. While the membrane invaginations of the small bud were not associated with cortical actin patches, they did appear occasionally to be labeled with anti-actin antibodies.

Ultrastructure of the Cortical Actin Patch

Yeast actin filaments, when assembled in vitro and examined in the electron microscope, have the usual diameter of ~7 nm (Greer and Schekman, 1982; Kilmartin and Adams, 1984). Occasionally, we observed filaments measuring ~7 nm to which actin antibodies localized (Fig. 9). Because cell sections are relatively thick, the best resolution of 7-nm filaments was obtained within cortical actin patches that had been longitudinally sectioned just above the plane of their plasma membrane core. These longitudinal sections reduced

Published April 1, 1994

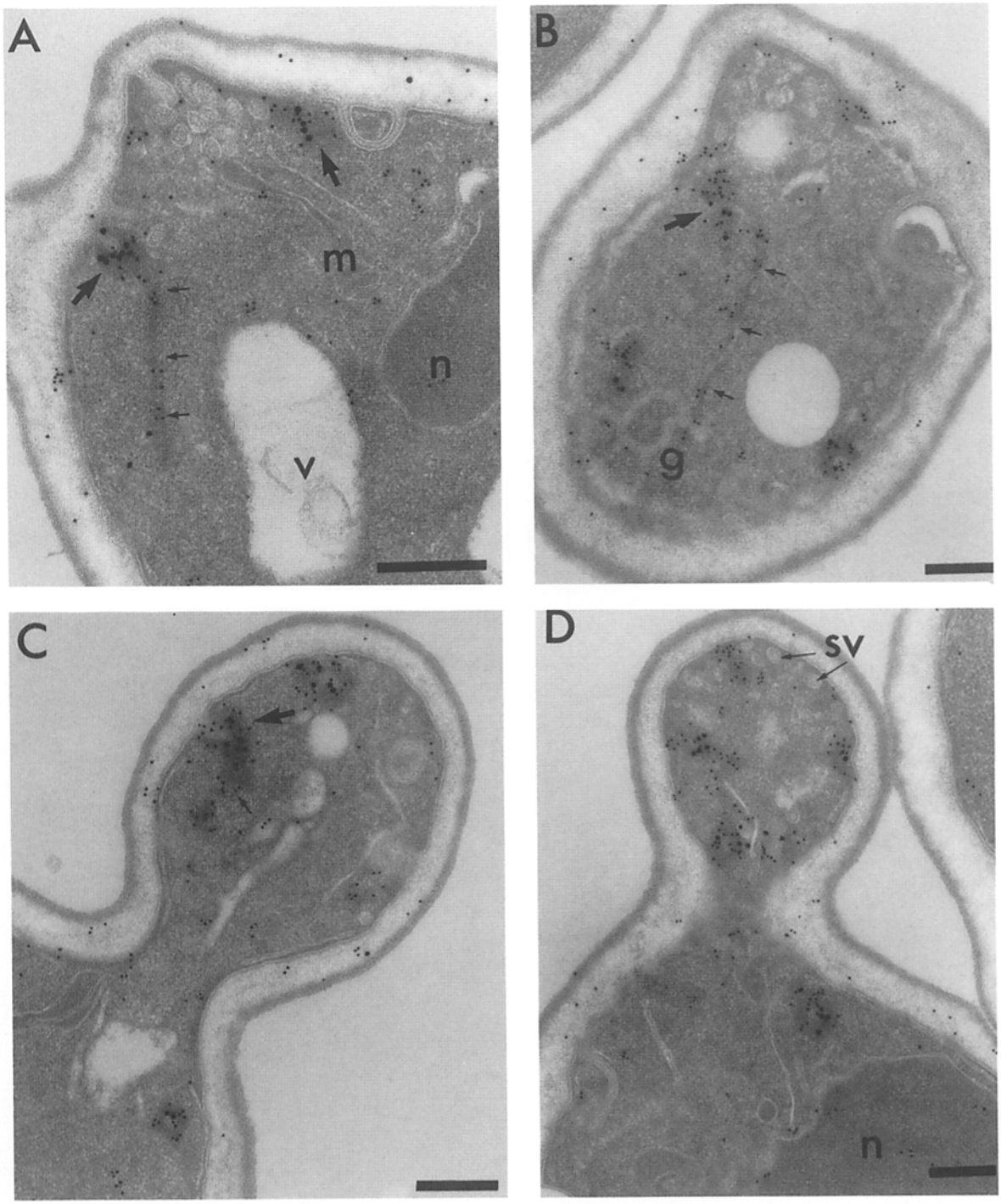

Figure 5. Localization of actin and Abplp. Abplp (20 nm gold) and actin (10 nm gold) colocalize to electron-dense, cell surface–associated cortical patches (*large arrows*) at the neck region of small buds (*A* and *B*). Actin alone is localized to the electron-dense cables (*small arrows*), which can be seen associated with the cortical patches. Cortical patches in larger buds also colocalize actin and Abplp (*C* and *D*). *m*, mitochondria; *n*, nucleus. *Bars*, 0.25 μm.

the amount of cellular material underlying the filaments and thus increased their resolution.

The 7-nm filaments observed within the cortical actin patch appeared to lie nearly perpendicular to the axis of plasma membrane invagination. Visualization of filaments in cross-sections through cortical patches proved difficult because of limited resolution between the thin 7-nm filaments and the surrounding cellular material. However, the pattern of anti-actin antibody localization on cross-sections through cortical patches often appeared ringlike (Fig. 9 *C*). Individual actin filaments could not be resolved within actin cables.

Discussion

Using immunoelectron microscopy, we localized actin and

Published April 1, 1994

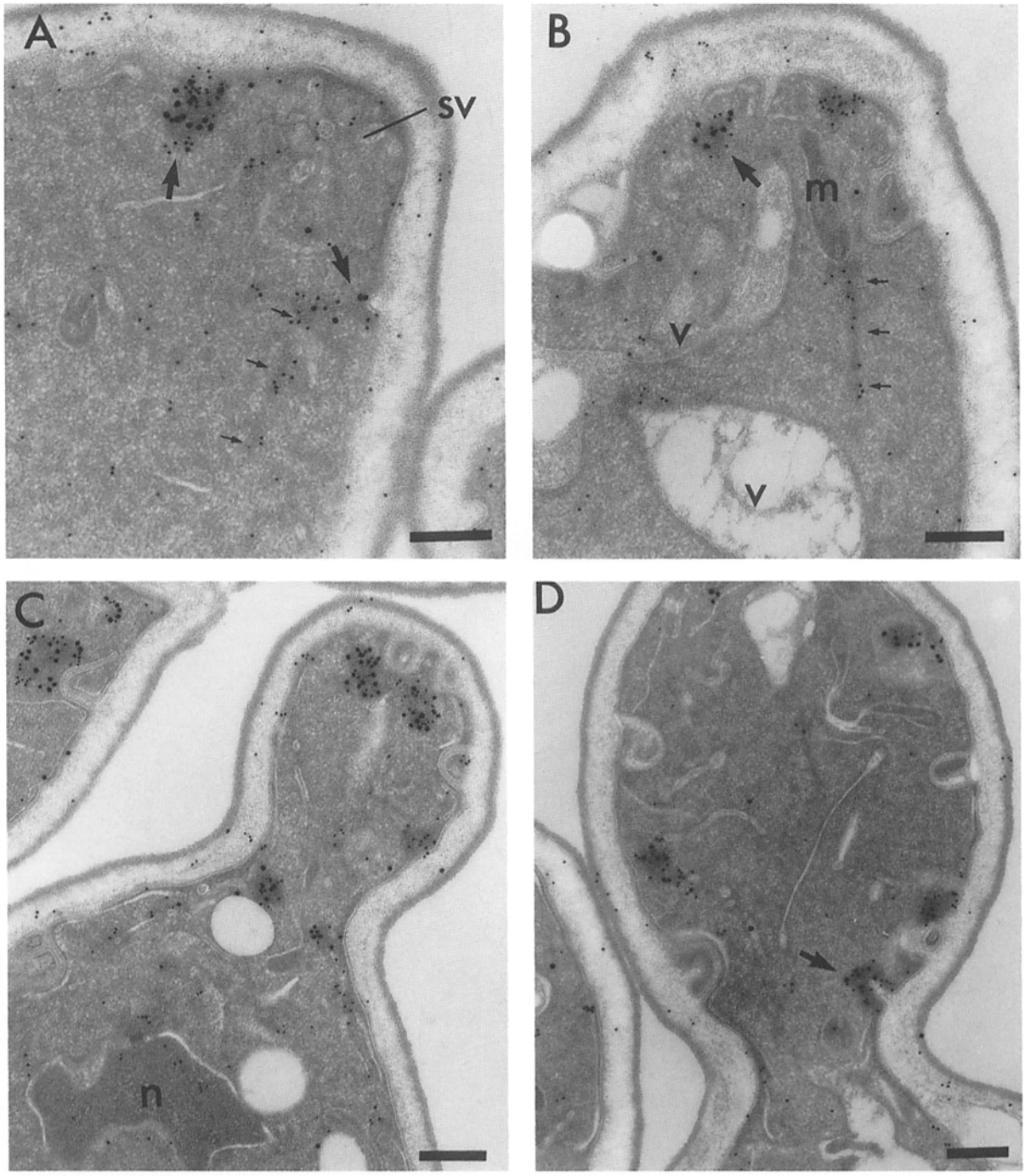

Figure 6. Localization of actin and cofilin. Cofilin (20 nm gold) and actin (10 nm gold) colocalize to electron-dense, cell surface–associated cortical patches (*large arrows*). Actin alone is localized to the electron-dense cables (*small arrows*), which can be seen associated with an actin cortical patch in a small budded cell (*A*), as well as aligned with a mitochondria (*B*). Actin and cofilin also colocalize to actin patches present in larger buds (*C* and *D*). *Bars*, 0.25 μm.

the actin-binding proteins Abp1p and cofilin to electron-dense cortical patches. This colocalization of actin with proteins known to reside specifically in the cortical cytoskeleton unequivocally identifies these structures as the ultrastructural equivalent of the brightly staining cortical patches observed in immunofluorescence light microscopy.

At the level of ultrastructure, we verified that the cortical actin patch is associated with the cell surface via an invagination of the plasma membrane. Filaments of appropriate diameter (ca. 7 nm) sometimes can be seen running more or less perpendicular to the axis of the plasma membrane invagination. Ringlike localization patterns of anti-actin antibodies can be observed on cross-sections through the cortical patch. We also regularly observed cables proximal to and possibly extending into the cytoplasm from cortical patches producing a characteristic bent elbow appearance (see Figs. 5, *A* and *B*, and 6 *A*).

The simplest interpretation of these observations is that

Published April 1, 1994

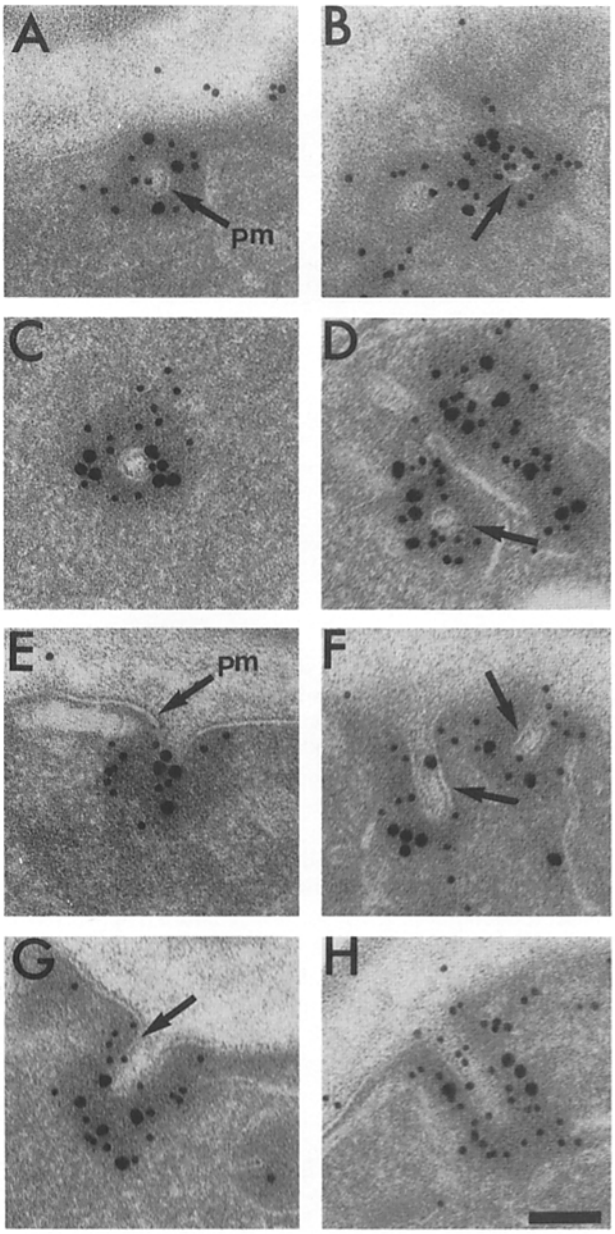

Figure 7. Cortical actin patches are associated with membrane. Putative cross-sections through cortical patches (*A–D*) reveal an electron-translucent core bounded by a ring of membrane (*arrows*), which is in turn surrounded by an electron-dense patch to which actin (10 nm gold) together with Abplp (20 nm gold) (*A*, *C*, and *D*) and cofilin (20 nm gold) (*B*) are colocalized. An association with an invagination of the plasma membrane and cell surface (*arrows*) is revealed in putative transverse sections through cortical patches (*E–H*). Plasma membrane invaginations are surrounded by electron-dense patches to which actin along with Abplp (*E*) and cofilin (*F–H*) are colocalized. *Bar*, 0.1 μm.

the actin cortical patch consists of a fingerlike invagination of the plasma membrane, around which actin filaments and associated proteins are organized. This organization might consist of an array of actin filaments that are coiled around the plasma membrane invagination and that are contiguous with the filaments of the actin cable. This interpretation is summarized in the cartoon/model diagrammed in Fig. 10.

However, because our current immunoelectron microscopy technique does not allow good resolution of actin filaments, we cannot prove that the filaments in the cables interact with or are contiguous with the material in the cortical patch. Further characterization of the ultrastructural organization of cortical actin patches using methods other than those used here will be necessary.

A Possible Role for the Actin Cytoskeleton in Cell Wall Growth and Osmotic Regulation

The association of the cortical actin cytoskeleton with invaginations of the yeast cell surface represents a heretofore undescribed connection between actin and the plasma membrane. No entirely analogous cortical structures have been observed in other eukaryotes. The unique structural attributes of the yeast cortical actin cytoskeleton might, therefore, reflect functional requirements specific to cell growth and morphogenesis in yeast and fungi in general.

Yeast cells produce and maintain a large osmotic gradient across their plasma membrane, resulting in turgor pressure. Like other organisms with cell walls (i.e., plants, bacteria and other fungi), yeast cells apparently use this turgor pressure to force wall expansion, allowing cell growth (Cosgrove, 1986; Ortega et al., 1989). The presence of a large internal pressure, however, presents a difficult biophysical problem for cell growth. For, while the cell wall contains the cell's turgor pressure, the breaking of covalent bonds necessary for the insertion of new wall, an essential step in growth, creates a situation that is predisposed to cell lysis. Thus, unlike higher eukaryotes, yeast cell growth requires localized deposition and insertion of cell wall under osmotically prohibitive conditions.

Like yeast, bacteria use localized deposition of cell wall to determine and produce cell shape and apparently use an osmotic gradient to drive cell growth. It has been postulated that growth of the bacterial cell surface must occur in an environment of low surface stress to avoid cell lysis (Koch, 1983, 1985, 1988; reviewed in Harold, 1990). Thus, the breaking of existing cell wall bonds required for intense, localized cell growth, such as the zonal growth exhibited by streptococci, must occur in an environment that reduces or negates the cell's osmotic pressure.

Streptococci solve this problem by forming an invaginated area of localized cell surface growth (Shockman at al., 1974; Koch, 1985). The wall grows locally within this invaginated septum. We propose that yeast might negate or reduce the cell's turgor pressure in the same way, by invaginating the cell surface wherever new wall material is being inserted. Because yeast exhibit polarized growth these invaginations would have to be established and maintained at regions of active growth within the nascent bud, as well as at the site of septum formation. As we have shown here by immunoelectron microscopy, and as was shown earlier by immunofluorescence microscopy (Adams and Pringle, 1984), these are the points at which cortical actin patches containing the membrane invaginations are found. The cortical actin cytoskeleton, therefore, is well positioned to play a primary role in establishing and maintaining localized membrane invaginations necessary for polarized wall growth.

Our suggestion of a role for the cortical actin cytoskeleton in avoiding the osmotic consequences of wall growth is supported by the observation that many, if not quite all mutant

Published April 1, 1994

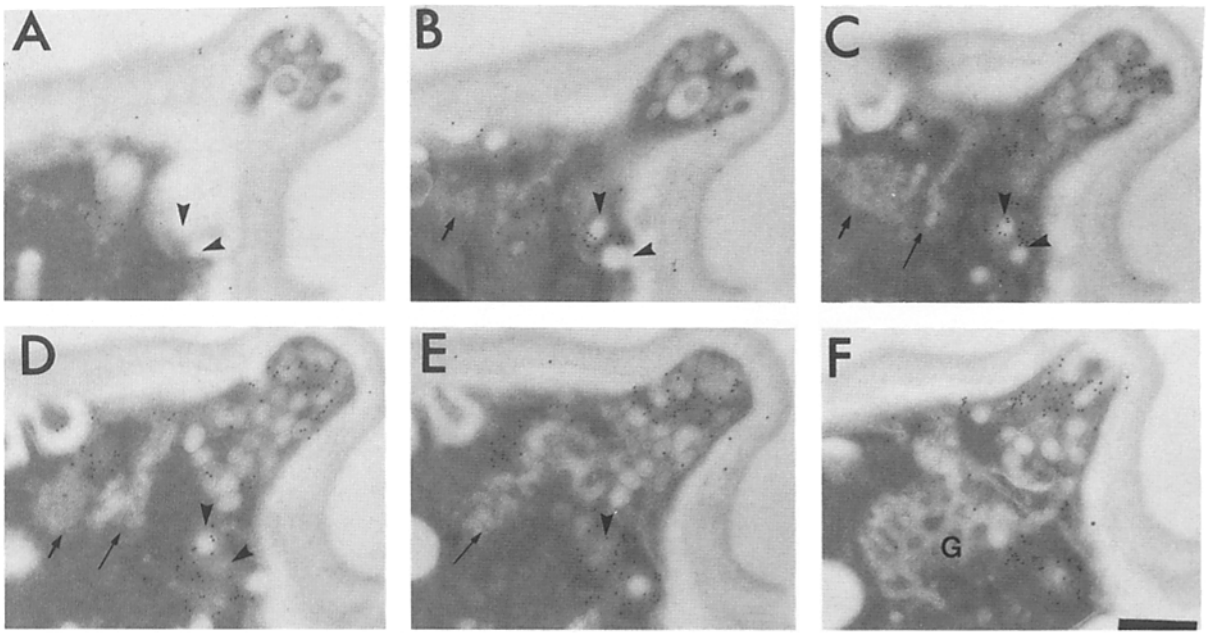

Figure 8. Serial section analysis of actin cortical patches immunolocalized with anti-actin antibodies. (*A–F*) A portion of a serial section through a ring of cortical patches localized at the neck of a small bud. Cell surface invaginations (*arrowheads*) associated with patches of cortical actin can be followed in serial section until they appear as electron-translucent cores surrounded by patches of cortical actin. Short and long arrows indicate aggregates of small (ca. 20 nm) and larger (ca. 30–40 nm) vesicles that are apparently associated with the Golgi structure seen in *F. Bar*, 0.25 μm.

actin alleles have been shown to confer upon cells substantial and characteristic increases in osmotic sensitivity (Novick and Botstein, 1985; Wertman et al., 1992; Drubin et al., 1994). Recently, Chowdhury et al. (1992) identified suppressors specifically for the osmotic sensitivity phenotype observed in *act1-1* and *act1-2*, identifying thereby at least one gene specifying a possible actin-binding protein. Thus the actin cytoskeleton, and not just actin, is implicated in controlling the osmotic sensitivity phenotype.

The hypothesis outlined above suggests that this sensitivity to osmotic pressure conferred by actin mutants can be explained simply in terms of defective assembly and/or attachment of the actin cytoskeleton to areas of the cell surface involved in wall growth. Defective cortical actin patches would not be able to adapt to changes in local surface stress at the site of cell wall insertion, as well as wild type patches. Alternatively, defective cortical actin patches may not provide adequate reductions in local surface tension. The presence of high surface tension at areas of growth would then result in compromised wall synthesis. In either case, changes in extra or intercellular osmolarity might result in a greater tendency for growing cells to leak (or even lyse) at the points that cell wall continuity is broken in the course of adding new material to the cell wall.

The Actin Cytoskeleton and Endocytosis

Recently, the actin cytoskeleton has been implicated in receptor-mediated endocytosis in yeast (Kubler and Riezman, 1993). The mutant actin alleles, *act1-1* and *act1-2*, as

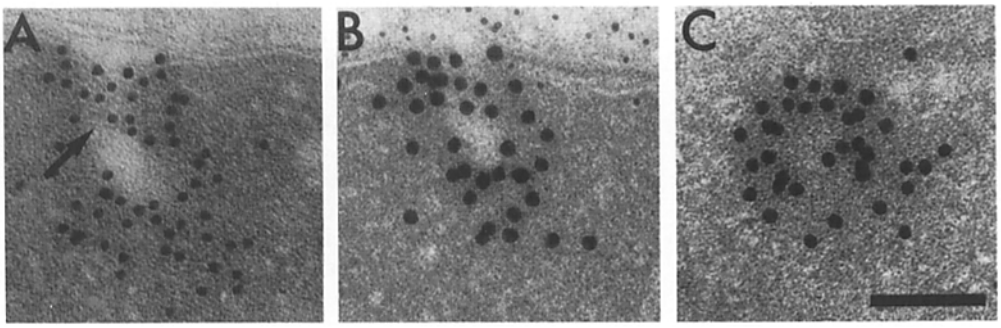

Figure 9. High magnification examination of the cortical actin patch. Ordered arrays of immunogold localized actin running almost perpendicular to the axis of the plasma membrane invagination can be seen on longitudinal sections through actin patches (*A* and *B*). In *A*, at least two labeled filaments (ca. 7 nm), which appear negatively stained, can be resolved (*arrow*). On cross-sections through the actin patch (*C*), immunolocalization of antibodies directed against actin produces ring-like patterns. *Bar*, 0.1 μm.

Published April 1, 1994

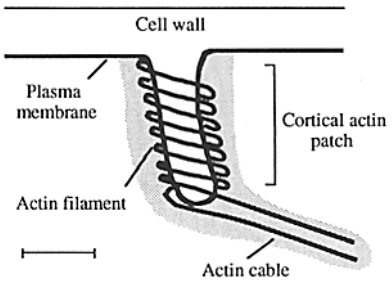

Figure 10. Cartoon of the cortical actin patch and its association with the cell surface, including a possible model for actin filament organization within the cortical actin patch and cable. *Bar*, 0.1 μm.

well as a disruption allele of *sac6*, the yeast homologue of vertebrate fimbrin, do not efficiently internalize the yeast mating pheromone α-factor. Yeast fimbrin has been shown to bundle actin filaments in vitro (Adams et al., 1991) and colocalizes with actin in vivo (Drubin et al., 1988). Kubler and Riezman (1993) hypothesize that organized bundles of actin filaments may be required to drive scission of vesicles from invaginations of the plasma membrane. Further, actin cables may be involved in producing the plasma membrane invaginations from which these endocytic vesicles are produced. Thus, it may well be that the association we have found between the actin cortical structure and the plasma membrane is the site of endocytosis. However, direct evidence for this is, as yet, entirely lacking.

We are indebted to Gilbert Keller and Mark Siegel of Genentech, Inc. (South San Francisco, CA) for extensive use of their Electron Microscopy Facility. We thank the members of the Botstein lab for useful discussion.

Research was supported by grants to D. Botstein from the National Institutes of Health (NIH) (GM-46406 and GM-46888) and to D. Drubin from the NIH (GM-42759) and the Searle Scholars/The Chicago Community Trust. D. Preuss was supported by a National Science Foundation Predoctoral fellowship.

Received for publication 3 January 1994 and in revised form 1 February 1994.

References

Adams, A. E. M., and J. R. Pringle. 1984. Relationship of actin and tubulin distribution in wild-type and morphogenetic mutant *Saccharomyces cerevisiae*. *J. Cell Biol.* 98:934–945.

Adams, A. E. M., D. Botstein, and D. Drubin. 1991. Requirement of yeast fimbrin for actin organization and morphogenesis in vivo. *Nature (Lond.).* 354:404–408.

Barnes, G., D. Drubin, and T. Streans. 1990. The cytoskeleton of *Saccharomyces cerevisiae*. *Curr. Opin. Cell Biol.* 2:109–115.

Burnette, W. N. 1981. "Western blotting": electrophoretic transfer of proteins from sodium dodecyl sulfate-polyacrylamide gels to unmodified nitrocellulose and autoradiographic detection with antibody and radioiodinated protein A. *Anal. Biochem.* 112:195–203.

Byers, B. 1981. Cytology of the yeast life cycle. *In* The molecular biology of the yeast saccharomyces. J. N. Strathern, E. W. Jones, and J. R. Broach, editors. Cold Spring Harbor Laboratory, Cold Spring Harbor, NY. pp. 59–96.

Chowdhury, S., K. W. Smith, and M. C. Gustin. 1992. Osmotic stress and the yeast cytoskeleton: phenotype-specific suppression of an actin mutation. *J. Cell Biol.* 118:561–571.

Cosgrove, D. 1986. Biophysical control of plant cell growth. *Annu. Rev. Plant Physiol.* 37:377–405.

Drubin, D. G., K. Miller, and D. Botstein. 1988. Yeast actin-binding proteins: evidence for a role in morphogenesis. *J. Cell Biol.* 107:2551–2561.

Drubin, D. G. 1991. Development of cell polarity in budding yeast. *Cell.* 65:1093–1096.

Drubin, D. G., H. Jones, and K. Wertman. 1994. Actin structure and function: roles in mitochondrial organization and morphogenesis in budding yeast and identification of the phalloidin-binding site. *Mol. Biol. Cell.* 4:1277–1294.

Field, C., and R. Schekman. 1980. Localized secretion of acid phosphatase reflects the pattern of cell surface growth in *Saccharomyces cerevisiae*. *J. Biol. Chem.* 254:796–803.

Glauert, A. M. 1975. *In* Practical Methods in Electron Microscopy. Vol. 3. North-Holland, Amsterdam. p. 46.

Greer, C., and R. Schekman. 1982. Actin from *Saccharomyces cerevisiae*. *Mol. Cell. Biol.* 2:1279–1286.

Harold, F. M. 1990. To shape a cell: an inquiry into the causes of morphogenesis of microorganisms. *Microbiol. Rev.* 54:381–431.

Kilmartin, J., and A. E. M. Adams. 1984. Structural rearrangements of tubulin and actin during the cell cycle of the yeast *Saccharomyces*. *J. Cell Biol.* 98:922–933.

Koch, A. L. 1983. The surface stress theory of microbial morphogenesis. *Adv. Microb. Physiol.* 24:301–366.

Koch, A. L. 1985. How bacteria grow and divide in spite of high internal hydrostatic pressure. *Can. J. Microbiol.* 31:1071–1083.

Koch, A. L. 1988. Biophysics of bacterial walls viewed as stress-bearing fabric. *Microbiol. Rev.* 52:337–353.

Kubler, E., and H. Riezman. 1993. Actin and fimbrin are required for the internalization step of endocytosis in yeast. *EMBO (Eur. Mol. Biol. Organ.) J.* 12:2855–2862.

Liu, H., and A. Bretscher. 1989. Disruption of the single tropomyosin gene in yeast results in the disappearance of actin cables from the cytoskeleton. *Cell.* 57:233–242.

Luna, E. J., and A. L. Hitt. 1992. Cytoskeleton-plasma membrane interactions. *Science (Wash. DC).* 258:955–964.

Matile, P., H. Moor, and C. F. Robinow. 1969. Yeast cytology. *In* The Yeasts. A. H. Rose and J. S. Harrison, editors. Academic Press, New York. pp. 219–302.

Moon, A. L., P. Janmey, K. A. Louie, and D. Drubin. 1993. Cofilin is an essential component of the yeast cortical cytoskeleton. *J. Cell Biol.* 120: 421–435.

Novick, P., and D. Botstein. 1985. Phenotypic analysis of temperature-sensitive yeast actin mutants. *Cell.* 40:405–416.

Ortega, J. K. E., E. G. Zehr, and R. G. Keanini. 1989. In vivo creep and stress relaxation experiments to determine the wall extensibility and yield threshold for sporangiophores of *Phycomyces*. *Biophys. J.* 56:465–475.

Preuss, D., J. Mulholland, C. A. Kaiser, P. Orlean, C. Albright, M. D. Rose, P. W. Robbins, and D. Botstein. 1991. Structure of the yeast endoplasmic reticulum: localization of ER proteins using immunofluorescence and immunoelectron microscopy. *Yeast.* 7:891–911.

Preuss, D., J. Mulholland, A. Franzusoff, N. Segev, and D. Botstein. 1992. Characterization of the *Saccharomyces* Golgi complex through the cell cycle by immunoelectron microscopy. *Mol. Biol. Cell.* 3:789–803.

Pringle, J. R., R. A. Preston, A. Adams, T. Streans, D. Drubin, B. Haarer, and E. Jones. 1989. Fluorescence microscopy for yeast. *Methods Cell Biol.* 31:357–435.

Reynolds, E. S. 1963. The use of lead citrate at high pH as an electron opaque stain in electron microscopy. *J. Cell Biol.* 17:208–212.

Sherman, F., G. R. Fink, and J. B. Hicks. 1986. Laboratory Course Manual for Methods in Yeast Genetics. Cold Spring Harbor Laboratory, Cold Spring Harbor, NY.

Shockman, G. D., L. Daneo-Moore, and M. L. Higgins. 1974. Problems of cell wall and membrane growth, enlargement and division. *Ann. NY Acad. Sci.* 235:161–196.

van Tuinen, E., and H. Reizman. 1987. Immunolocalization of glyceraldehyde-3-phosphate dehydrogenase, hexokinase, and carboxypeptidase Y in yeast cells at the ultrastructural level. *J. Histochem. Cytochem.* 35:327–333.

Wertman, K., D. G. Drubin, and D. Botstein. 1992. Systemic mutational analysis of the yeast *ACT1* gene. *Genetics.* 132:337–350.

Wright, R., and J. Rine. 1989. Transmission electron microscopy and immunocytochemical studies of yeast: Analysis of HMG-CoA reductase overproduction by electron microscopy. *Methods Cell Biol.* 31:473–512.

Yaffe, M. P. 1991. Organelle inheritance in the yeast cell cycle. *Trends Cell Biol.* 1:160–164.

Zechel, K. 1980. Isolation of polymerization-competent cytoplasmic actin by affinity chromatography on immobilized DNase I using formamide as elutant. *Eur. J. Biochem.* 110:343–348.